

Stabilizing the Homopolycation $(I_4)^{2+}$ with a Hexasulfate in $(I_4)[S_6O_{19}]$ and a Borosulfate in $(I_4)[B(S_2O_7)_2]_2$

David van Gerven, Stefan Sutorius, Jörn Bruns,* and Mathias S. Wickleder*^[a]

The reaction of elemental iodine and SO_3 in a sealed glass ampoule yielded a turquoise-colored solution. At temperatures below $7^\circ C$, deep red crystals of $(I_4)[S_6O_{19}]$ grow. With the addition of B_2O_3 and pyridine- SO_3 complex red crystals of $(I_4)[B(S_2O_7)_2]_2$ can be obtained after heating the mixture to

$120^\circ C$. The combination of an $(I_4)^{2+}$ cation with oxoanions has previously not been observed. Both anions have a significant but different influence on the structural properties of the $(I_4)^{2+}$ cation.

Introduction

The formation of red and green coloured solutions when concentrated sulfuric acid reacts with tellurium and selenium, respectively, is well known and a typical show experiment in freshman courses. In fact, these reactions can be traced back to the early days of chemistry and Klaproth was the first to report the tellurium reaction.^[1,2] Today we know that the observed colour is caused by the formation of polycations, in this case $[Te_4]^{2+}$ and $[Se_8]^{2+}$, respectively.^[3,4] Moreover, quite a number of further chalcogen polycations have been reported up to date, significantly inspired by the work of Gillespie et al. in the early 1970s.^[5,6] Interestingly, most of these cations are not stabilized as oxoanionic salts, although their discovery originates from reactions in sulfuric acid. Usually the polycations are crystallized as fluoro-antimonates or -arsenates, and $(Se_4)[HS_2O_7]$, obtained from Se and oleum, is one of the few exceptions.^[7] The early discovery of chalcogen cations has certainly triggered investigations aiming at the preparation of similar cations, including the heavier halogens. Thus, the observation of iodine cations was also reported more than 80 years ago.^[8] Meanwhile, several polyiodine cations such as I_3^+ and I_5^+ have been identified, however, again, not as sulfates or polysulfates, but as $[AsF_6]^-$ and $[SbF_6]^-$ salts, respectively.^[9-13] The reason for the preference of the anions is, on the one hand that they are weak ligands and on the other, the respective pentafluorides AsF_5 and SbF_5 are suitable oxidizers which allow oxidation of the heavier chalcogens and halogens in a defined way. Moreover, the pentafluorides can be used in liquid SO_2 as a solvent, so that

crystallization is facilitated. Another oxidant that has gained popular interest for the preparation of halogen polycations is peroxydisulfuryl difluoride, $S_2O_6F_2$. After oxidation it provides the $[SO_3F]^-$ anion for the stabilization of the generated polycations.^[14] In the case of iodine the reaction leads to the $(I_2)^+$ cation, however, some disproportionation to $(I_3)^+$ and $I(SO_3F)_3$ is observed.^[15] Furthermore, there was clear evidence that the I_2^+ cation undergoes dimerization under formation of a $(I_4)^{2+}$ cation at lower temperature in this medium.^[16] Optically, the dimerization is accompanied by a colour change of the solution from dark blue to red upon cooling. The $(I_4)^{2+}$ cation has later been isolated in the solid state, namely in form of the salts $(I_4)[AsF_6]_2$, $(I_4)[SbF_6]_2$, and $(I_4)[Sb_3F_{14}][SbF_6]$.^[17] It is noteworthy to mention, that this cation also has not been stabilized in an oxoanionic environment. In general, it can be summarized that the preparation and stabilization of chalcogen and halogen polycations is best achieved using a combination of a sufficiently powerful oxidizer and a weak coordinating anion of a superacid. In retrospect, the initial observations that resulted from experiments in H_2SO_4 and H_2SO_4/SO_3 mixtures (oleum) are consistent, as these media meet the requirements perfectly. Furthermore, the combination of iodine and oleum (65% SO_3) has been investigated as a potential medium.^[18,19] The formation of a blue solution has been reported but crystallization attempts were strongly hampered by the viscosity of the solution.

In course of our investigations of the H_2SO_4/SO_3 system we reported several important findings. Firstly, the extraordinary oxidation power could be shown by the oxidation of platinum metals leading to several unique compounds.^[20-30] Secondly, we could demonstrate that the assumed infinite chain growth of polysulfuric acids $H_2S_nO_{3n+1}$, that is with increasing SO_3 content, is doubtful.^[31,32] Nevertheless, the assumption that the Brønsted acidity of H_2SO_4/SO_3 mixtures increases with increasing SO_3 content seems reasonable.^[33] Thus, we once more investigated the oxidation of iodine in this medium. In particular, we choose the reaction of I_2 with SO_3 as the initial experiment. It is known that liquid γ - SO_3 (mp. $16.8^\circ C$) is extremely prone to polymerization in the presence of water, even at very low H_2O concentrations ($> 10^{-6}$ mol%).^[34] Therefore, the reaction should

[a] Dr. D. van Gerven, S. Sutorius, Dr. J. Bruns, Prof. M. S. Wickleder
University of Cologne
Institute of Inorganic Chemistry
Greinstr. 6, 50939 Cologne (Germany)
E-mail: j.brun@uni-koeln.de
mathias.wickleder@uni-koeln.de

Supporting information for this article is available on the WWW under <https://doi.org/10.1002/open.202200122>

© 2022 The Authors. Published by Wiley-VCH GmbH. This is an open access article under the terms of the Creative Commons Attribution Non-Commercial NoDerivs License, which permits use and distribution in any medium, provided the original work is properly cited, the use is non-commercial and no modifications or adaptations are made.

provide a long chained polysulfate anion, as SO_3 is most certainly a sufficiently strong oxidizer.

Results and Discussion

The reaction was carried out in such a fashion that elemental iodine and SO_3 were heated to 80°C in a sealed glass ampoule. Upon cooling to room temperature, a homogeneous turquoise coloured solution was obtained (see Figure S1 in the Supporting Information). After storing the ampoule in a refrigerator at a temperature below 7°C , a large number of red crystals grew. The agglomerates of these crystals were located next to needle shaped asbestos type SO_3 crystals, which grew simultaneously. Prosaically speaking, the red crystals appear as blossoms at the branches formed by asbestos type SO_3 crystals (Figure 1). The red crystals disappeared if the ampoule is warmed above 7°C . Moreover, they decompose rapidly after opening of the ampoule, even at low temperature. Thus, the manipulation of the single crystals and their preparation for the measurement has to occur rapidly and under keeping under constant cooling

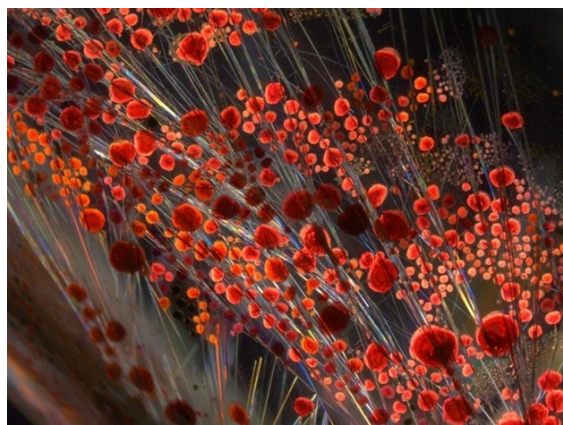


Figure 1. Red spherical single crystals of $(\text{I}_4)[\text{S}_6\text{O}_{19}]$ along with needle-shaped colourless crystals of asbestos type SO_3

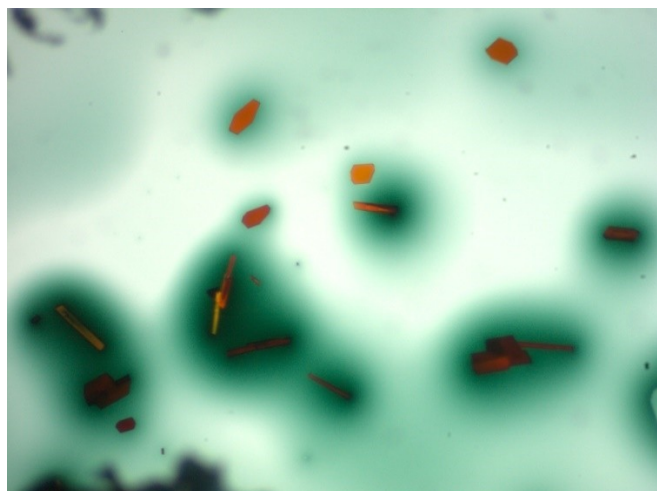


Figure 2. Red single crystals of $(\text{I}_4)[\text{B}(\text{S}_2\text{O}_7)_2]_2$.

(see Supporting Information). Finally, a single crystal could be measured at the P24 beamline at the DESY facility in Hamburg. The structure analysis revealed that $(\text{I}_4)[\text{S}_6\text{O}_{19}]$ has formed.

Neither reducing the amount of SO_3 nor increasing the temperature of the afore introduced mixture led to another product. Thus, with the aim of studying the cation with another anion that still features a polysulfate fragment of the chain, we managed to stabilize the $(\text{I}_4)^{2+}$ cation with a borosulfate anion, namely the *bis*-disulfatoborate anion $[\text{B}(\text{S}_2\text{O}_7)_2]^-$. As for $(\text{I}_4)[\text{S}_6\text{O}_{19}]$, elemental iodine was the starting material and was heated with a mixture of SO_3 , B_2O_3 and the pyridine- SO_3 complex (py-SO_3) to 120°C . $(\text{I}_4)[\text{B}(\text{S}_2\text{O}_7)_2]_2$ does not crystallize directly from the homogeneous turquoise coloured solution while cooling. However, several days later after having inverted the ampoule, red crystals could be observed on the inner wall (Figure 2).

It is the first time that the $(\text{I}_4)^{2+}$ cation could be isolated in form of oxoanionic salts. Interestingly, the stability of the structure results not only from the monovalent anion $[\text{B}(\text{S}_2\text{O}_7)_2]^-$ but also thanks to a divalent hexasulfate anion. To date, especially weakly coordinating monovalent anions of superacids were considered as ideal candidates. However, our findings corroborate the above-mentioned theoretical predictions, that the acidity of polysulfuric acids $\text{H}_2\text{S}_n\text{O}_{3n+1}$ increases with growing chain lengths. In fact, $(\text{I}_4)[\text{S}_6\text{O}_{19}]$ is only the third example of a compound containing the hexasulfate anion. The first observations were reported recently with the examples of $\text{Rb}_2[\text{S}_6\text{O}_{19}]$ and $(\text{NH}_4)_2[\text{S}_6\text{O}_{19}]$ by ourselves.^[32] Not unknown but also rare is the $[\text{B}(\text{S}_2\text{O}_7)_2]^-$ anion. Examples are known, for example, for the alkaline metals and silver in $M[\text{B}(\text{S}_2\text{O}_7)_2]$ ($M = \text{Li}, \text{Na}, \text{K}, \text{Ag}$).^[35,36,37] and even more recently we reported on two highly untypical heteropoly Au-Cl cations stabilized by $[\text{B}(\text{S}_2\text{O}_7)_2]^-$ anions.^[38]

As described for the fluorides $(\text{I}_4)[\text{AsF}_6]_2$, $(\text{I}_4)[\text{SbF}_6]_2$, and $(\text{I}_4)[\text{Sb}_3\text{F}_{14}][\text{SbF}_6]$, respectively, the $(\text{I}_4)^{2+}$ cation in both compounds has a rectangular shape with two short and two longer bonds (Figure 3). In $(\text{I}_4)[\text{S}_6\text{O}_{19}]$ the short bonds show a value of $260.8(3)$ pm while the longer edge of the rectangle is $322.1(1)$ pm long. The values are identical for two of the four bonds because the $(\text{I}_4)^{2+}$ cation is situated on the $4d$ site of space group $\text{C}2/c$, that is, it exhibits inversion symmetry. The respective bond lengths for the three fluorides are smaller for the short edge of the rectangle ($\varnothing = 258$ pm) and larger for the longer edge ($\varnothing = 327$ pm). In $(\text{I}_4)[\text{B}(\text{S}_2\text{O}_7)_2]_2$ two opposite bonds are identical and reveal values of $259.2(2)$ pm. The other two I–I distances are $308.7(2)$ pm and $339.8(3)$ pm, meaning they are not identical as in $(\text{I}_4)[\text{S}_6\text{O}_{19}]$. This finding can be explained by the coordination sphere around the $(\text{I}_4)^{2+}$ cations, which is very different in the two compounds. Similar to the reported fluorides, there is one shorter contact for each of the iodine atoms to the surrounding anions in $(\text{I}_4)[\text{S}_6\text{O}_{19}]$. In this case the respective distances I–O are found at $277.8(4)$ and $276.3(4)$ pm and all others are significantly larger than 300 pm. The situation is different for $(\text{I}_4)[\text{B}(\text{S}_2\text{O}_7)_2]_2$. While the shortest I–O distance for two of the four iodine atoms stems from a μ_1 -oxygen atom (I–O: $276.6(3)$ and $279.6(3)$ pm), the other two result from a μ_2 -coordinating oxygen atom (I–O: $294.4(3)$, $297.3(3)$ pm). The two

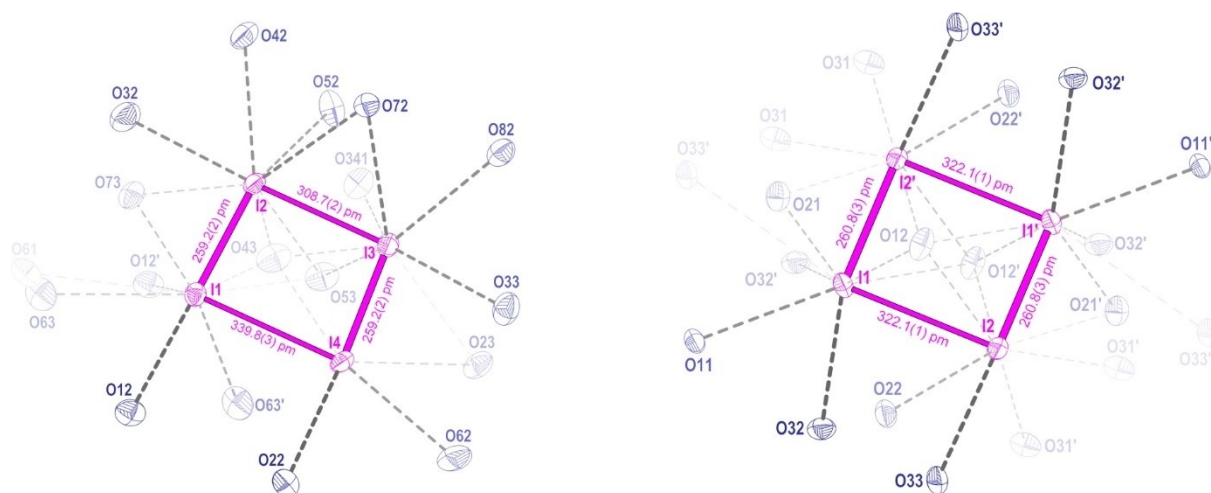


Figure 3. Left: Surrounding of the $(I_4)^{2+}$ cation in $(I_4)[B(S_2O_7)_2]_2$; Right: Surrounding of the $(I_4)^{2+}$ cation in $(I_4)[S_6O_{19}]$. The thermal ellipsoids are set at 70% probability. For selected bond lengths see Table 1 and the Supporting Information.

iodine atoms that are coordinated by the μ_2 -oxygen atom have two and three additional I–O connections with only little more than 300 pm distance, respectively.

In principle, the formation and the structure of the $(I_4)^{2+}$ cation is theoretically well understood: In a first step the oxidation of the I_2 molecule leads to shortening of the I–I bond under formation of an $(I_2)^+$ cation. The latter shows an unpaired electron in a π^* orbital and pairing of two of these radicals leads to the $(I_4)^{2+}$ ion (see also Supporting material).^[39–41]

$(I_4)[S_6O_{19}]$ is the third example for the existence of the hexasulfate anion. In previous reports we have shown that the stability of polysulfate anions $[S_nO_{3n+1}]^{2-}$ against loss of SO_3 decreases with growing numbers of n . This decreasing stability is strongly correlated with the increasing distance of the terminal S–O bond within the backbone of the anion. The longer the polysulfate chain grows the more the anion can be seen as a Lewis acid/base adduct of the respective smaller polysulfate anion. For the hexasulfate anions in $Rb_2[S_6O_{19}]$ and $(NH_4)_2[S_6O_{19}]$ bond lengths S–O as long as 220.49(6) and even 230.9(1) pm are found, justifying a formulation according to $[S_5O_{16}]^{2-} \cdot SO_3$.^[32] The situation for the hexasulfate ion in $(I_4)[S_6O_{19}]$ is significantly different. It is still observed that the terminal sulfur oxygen bond (S3–O231) is the longest within the anion, however, with a value of 177.6(4) pm this bond is dramatically shorter than that found for the rubidium and ammonium compounds, respectively (Figure 4). The difference of more than 40 pm is remarkable and the observed distance is also significantly shorter than the value predicted by theory (195.3).^[32,42] Even if the data known so far is scarce, there seems to be clear evidence that the nature of the respective counter cation has a great influence on the bond lengths observed in the hexasulfate anion. The cation in $(I_4)[S_6O_{19}]$ is highly unusual compared to the spherical ions used so far. The $(I_4)^{2+}$ cation is connected by only two quite short bonds involving the atoms O32 and O33 of the terminal $[SO_4]$ groups of the $[S_6O_{19}]^{2-}$ ion (Figure 4 and 5). We assume that these moieties donate electron density to the π^* -orbital of the respective $(I_2)^+$ units,

Table 1. Selected bond length for $(I_4)[B(S_2O_7)_2]_2$ and $(I_4)[S_6O_{19}]$.

$(I_4)[B(S_2O_7)_2]_2$ bond	atom distance [pm]	$(I_4)[S_6O_{19}]$ bond	atom distance [pm]
I1–I2	259.2(7)	I1–I2	322.1(1)
I1–I4	339.8(3)	I1–I2'	260.8(3)
I2–I3	308.7(2)	I1'–I2	260.8(3)
I3–I4	259.2(2)	I1'–I2'	322.1(1)
I1–O12	279.6(3)	I1–O11	306.4(4)
I1–O12'	305.0(5)	I1–O12	343.8(4)
I1–O43	363.7(3)	I1–O12'	352.4(4)
I1–O53	368.8(3)	I1–O21	342.1(4)
I1–O61	366.9(3)	I1–O32	276.3(4)
I1–O63	345.9(4)	I1–O32'	348.6(4)
I1–O63'	328.9(3)		
I1–O73	341.5(3)		
I2–O32	304.7(3)	I2–O12	348.9(4)
I2–O42	306.8(3)	I2–O12'	344.7(4)
I2–O43	354.4(3)	I2–O22	326.2(4)
I2–O52	321.9(3)	I2–O31	356.3(4)
I2–O53	350.2(3)	I2–O31'	362.9(4)
I2–O72	297.3(3)	I2–O33	277.8(4)
I2–O73	349.7(3)	I2–O21'	364.0(4)
I3–O23	368.2(3)		
I3–O33	305.7(3)		
I3–O43	355.5(3)		
I3–O53	345.4(3)		
I3–O72	294.4(3)		
I3–O82	303.7(3)		
I3–O341	349.9(3)		
I4–O22	276.6(3)		
I4–O23	352.3(3)		
I4–O43	358.8(3)		
I4–O53	370.1(3)		
I4–O62	312.5(3)		

causing the significantly different I–I distances of the $(I_4)^{2+}$ cation. These strong interactions are also reflected by the bond lengths S3–O32 and S3–O33 (144.6(4) and 144.1(4) pm) which are significantly longer than those observed in the hexasulfate anions known so far (≈ 140 pm).

In contrast to $(I_4)[S_6O_{19}]$, which exhibits a comparatively symmetrical surrounding of the $(I_4)^{2+}$ cation, the coordination sphere of the $(I_4)^{2+}$ cation in $(I_4)[B(SO_4)_2]_2$ is highly unsym-

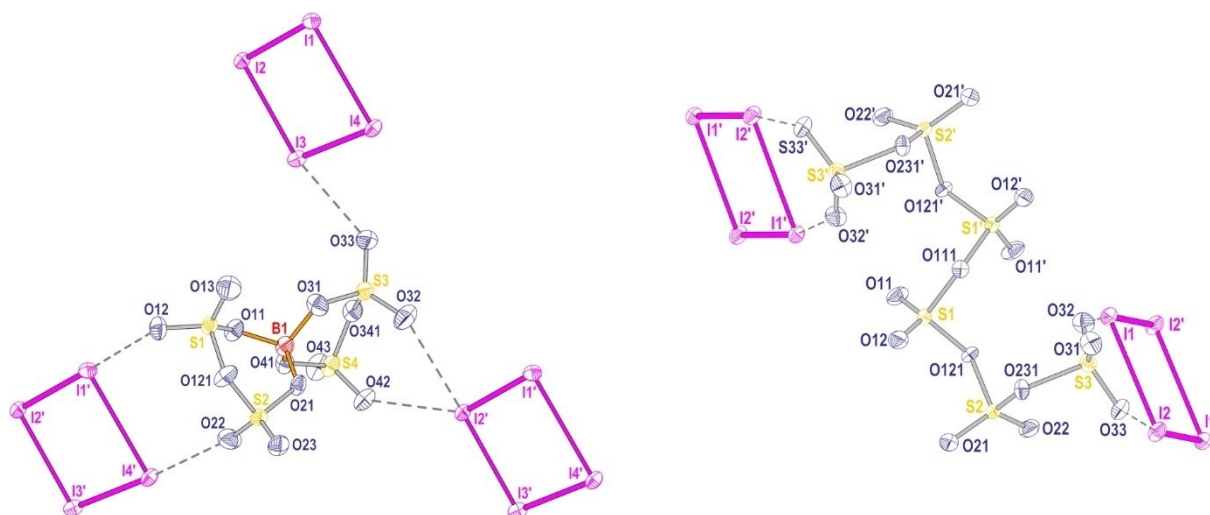


Figure 4. Left: The $[B(S_2O_7)_2]^-$ anion in $(I_4)[B(S_2O_7)_2]_2$; Right: The $[S_6O_{19}]^{2-}$ ion in $(I_4)[S_6O_{19}]$. The thermal ellipsoids are set at 70% probability. Selected bond lengths for one of the two crystallographically different $[B(S_2O_7)_2]^-$ anions in pm: S1–O11: 152.7(3), S1–O12: 142.0(3), S1–O13: 140.1(3), S1–O21: 162.4(3), S2–21: 152.5(3), S2–O22: 141.7(3), S2–O23: 140.2(3), S2–O121: 161.7(3), S3–O31: 152.6(3), S3–O32: 141.0(3), S3–O33: 140.7(3), S3–O341: 161.9(3), S4–O41: 152.6(3), S4–O42: 141.7(3), S4–O43: 140.8(3), S4–O341: 163.4(3); Selected bond lengths for the $[S_6O_{19}]^{2-}$ ion in pm: S1–O111: 162.4(3), S1–O121: 157.6(4), S1–O11: 141.2(4), S1–O12: 140.3(4), S2–O231: 153.8(4), S2–O121: 167.4(4), S2–O21: 141.2(4), S2–O22: 141.4(4), S3–O231: 177.6(4), S3–O32: 144.6(4), S3–O33: 144.1(4), S3–O31: 141.9(4). Full data are given in the Supporting Information.

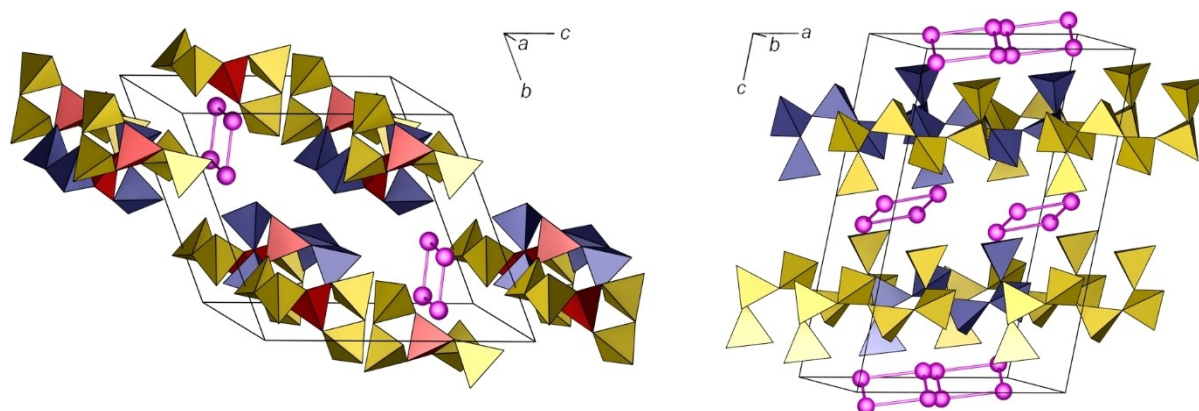


Figure 5. Left: Arrangement of $(I_4)^{2+}$ cations and $[B(S_2O_7)_2]^-$ anions in the crystal structure of $(I_4)[B(S_2O_7)_2]_2$; Right: Arrangement of I_4^{2+} cations and $[S_6O_{19}]^{2-}$ anions in the crystal structure of $(I_4)[S_6O_{19}]$. For clarity the anions ions are drawn in a polyhedral style and with different colours although crystallographically they are identical. Color code: pink – $(I_4)^{2+}$, yellow – (SO_4) , red – (BO_4) , blue – the respective anions behind.

metrical. The different borosulfate anions seem to dictate the structure of the cation. Thus, the longest I–I distance (339.8(3) pm), which is significantly longer than the longest I–I distance in $(I_4)[S_6O_{19}]$ (322.1(1) pm), is coordinated only by one chelating borosulfate anion with short I–O distances of (259.2(2) and 259.2(7) pm). As for $(I_4)[S_6O_{19}]$ further I–O contacts values > 300 pm can be found. Thus, this finding resembles the situation seen for the hexasulfate anions, in particular exhibiting only chelating μ_1 -oxygen coordination. However, the opposite side of the $(I_4)^{2+}$ cation in $(I_4)[B(SO_4)_2]_2$ exhibits μ_2 -oxygen coordination and multiple further contacts to terminal oxygen atoms of borosulfate anions with distances close to 300 pm. Thus, the I–I distance reveals a value of only 308.7(2) pm. The S–O bond lengths of the borosulfate anions are similar to findings for species with spherical monoatomic cations. Thus, the coordination of the borosulfate anion to the $(I_4)^{2+}$ cation

causes no change in the Lewis acidity of the anion, which is in contrast to the findings for the hexasulfate, where the coordination has a strong influence on the structure of the anion. However, the more compact structure of the borosulfate favours the higher coordination number of the $(I_4)^{2+}$ cation and thus influences the bonding situation of the cation significantly.

Conclusions

The successful preparation and characterization of $(I_4)[S_6O_{19}]$ and $(I_4)[B(S_2O_7)_2]_2$ provides both, first examples of the $(I_4)^{2+}$ cation in an oxoanionic environment and new versions of the rarely seen anions $[B(S_2O_7)_2]^-$ and $[S_6O_{19}]^{2-}$, displaying remarkable differences with respect to the hexasulfates known so far. Besides these fundamental findings, the investigations illustrate

once more the enormous potential of SO_3 for the preparation of unusual species. In particular, it seems that further scrutiny of non-metallic element reactions in SO_3 is worthy of consideration.

Experimental Section

Synthesis

SO_3 was obtained in a specially designed apparatus for the generation, distillation and the subsequent transfer into glass ampoules under nitrogen gas. For this purpose, fuming sulfuric acid (5 mL, 65% SO_3 , used as received, Merck, Darmstadt, Germany) was slowly added via a dropping funnel into a 500 mL flask with P_4O_{10} (250 g, >97%, Merck, Darmstadt). At the same time, the flask was heated at 130 °C and the generated SO_3 distilled into a connected burette body (scaling 0.01 mL \pm 0.01). A connected glass ampoule ($l=200$ mm, $\phi=20$ mm, thickness of the tube wall = 2 mm) containing the solid starting materials was then filled with the suitable amount of SO_3 . In the case of $(\text{I}_4)[\text{S}_6\text{O}_{19}] \text{I}_2$ powder (253 mg, Riedel-de Haën, Seelze) was used and the ampoule then filled with 1.00 mL (24.5 mmol) of freshly distilled SO_3 . In the case of $(\text{I}_4)[\text{B}(\text{S}_2\text{O}_7)_2]_2$ the pyridine- SO_3 complex (284 mg, Sigma Aldrich, Hamburg) was added to I_2 powder (150 mg, Riedel-de Haën, Seelze) and B_2O_3 powder (105 mg, Sigma Aldrich, Hamburg). The powders were not ground together in a mortar. The ampoule was then filled with 0.55 mL (14.0 mmol) of freshly distilled SO_3 . The ampoules were torch sealed and heated in a tube furnace. For the synthesis of $(\text{I}_4)[\text{S}_6\text{O}_{19}]$ a maximum temperature of 80 °C is required, for $(\text{I}_4)[\text{B}(\text{S}_2\text{O}_7)_2]_2$ the reaction temperature is 120 °C. The respective temperatures were maintained for 48 h and the reaction mixtures were then allowed to cool to room temperature at rate of 1/3 °C h⁻¹ for $(\text{I}_4)[\text{S}_6\text{O}_{19}]$ and 1 °C h⁻¹ for $(\text{I}_4)[\text{B}(\text{S}_2\text{O}_7)_2]_2$, respectively. A homogeneous deep turquoise colored solution was obtained in both cases, from which red crystals crystallized in the refrigerator at 4 °C next to asbestos-like SO_3 needles in the case of $(\text{I}_4)[\text{S}_6\text{O}_{19}]$ and after turning the ampoule upside down after several days for $(\text{I}_4)[\text{B}(\text{S}_2\text{O}_7)_2]_2$ besides a colourless by-product. Above 7 °C, the red hexasulfate decomposes within a few minutes and can be re-crystallized again within several days in the refrigerator. The borosulfate is stable at ambient temperature in the closed ampoule. Opening of the ampoule leads to rapid decomposition of the obtained phases. Obviously, the surrounding SO_3 atmosphere seem to contribute essentially to the stability of the obtained phases.

Caution! SO_3 is a strong oxidizer, which needs careful handling. During the reaction and even after cooling down to room temperature the glass tubes may be pressurized. The tubes should be cooled with liquid nitrogen before opening.

Structure determination

$(\text{I}_4)[\text{S}_6\text{O}_{19}]$: Crystal structure determination was performed on the P24.1 beamline of the PETRA III facility at German Electron Synchrotron (DESY) Hamburg (Germany). The reaction ampoule containing the red crystalline phase of $(\text{I}_4)[\text{S}_6\text{O}_{19}]$ was stored in the refrigerator at 4 °C until shortly before the measurement. After opening the ampoule, single crystals were transferred to an inert oil with pre-cooled preparation equipment. By continuous cooling in a cold nitrogen stream the individual crystals were separated with the help of a light microscope polarizing filter. Despite the elaborate cooling efforts, the crystals showed spontaneous decomposition on contact with the micromount.

However, due to the surface tension of the inert oil used, a single crystal could be held in the centre of a larger micromount loop without directly touching its edges. Under constant cooling in liquid nitrogen, the attached single crystal was transferred to the cold nitrogen gas stream (100.0(2) K) of the single-crystal diffractometer (Huber 4-circle Kappa, P24 Beamline, Petra III) and intensity data was collected. Later attempts to measure the crystal at higher temperatures led to the loss of the single crystal above 250 K. This observation may be explained by either the temperature or the intensity of the synchrotron radiation used. We favour the first explanation, since all other crystals were likewise decomposed after a few minutes to form a red solution despite cooling under inert oil. We also assume that the obtained crystalline phase of $(\text{I}_4)[\text{S}_6\text{O}_{19}]$ is in fact stabilized within the SO_3 atmosphere of the closed ampoule at temperatures < 7 °C. The collected intensity data were reduced, and a cell refinement was carried out.^[43] Intrinsic phasing (ShelXT) gave a successful structure solution.^[44] Finally, anisotropic displacement parameters were introduced, and a multi-scan absorption correction was applied to the reflection data.^[43]

$(\text{I}_4)[\text{B}(\text{S}_2\text{O}_7)_2]_2$: Under a polarization microscope, a suitable crystal was prepared, mounted onto a micromount (MicroMounts™, MiTeGen LLC, New York, USA) and immediately placed into a stream of cold N_2 (100(2) K) inside the diffractometer (Bruker Photon III, Bruker, Karlsruhe, Germany). After unit cell determination, the reflection intensities were collected. The collected intensity data were reduced, and a cell refinement was carried out.^[43] The structure solution was successful using intrinsic phasing (SHELXT).^[44] Finally, anisotropic displacement parameters were introduced, and a multi-scan absorption correction was applied to the reflection data.^[43]

Atomic positions and further details of the crystal structures are given in the Supporting Information. Deposition Number(s) 1955943 (for $(\text{I}_4)[\text{S}_6\text{O}_{19}]$) and 2149733 (for $(\text{I}_4)[\text{B}(\text{S}_2\text{O}_7)_2]_2$) contain(s) the supplementary crystallographic data for this paper. These data are provided free of charge by the joint Cambridge Crystallographic Data Centre and Fachinformationszentrum Karlsruhe Access Structures service.

Acknowledgement

We acknowledge DESY (Hamburg, Germany), a member of the Helmholtz Association HGF, for the provision of experimental facilities. Parts of this research were carried out at PETRA III and we would like to thank Carsten Paulmann and Heiko Schulz-Ritter for assistance in using the P24 EH1 X-ray Diffraction Kappa-diffractometer. J.B. is thankful to the Fonds der Chemischen Industrie for financial support. André Santos Martinez is also to be thanked for his help in the sample preparation.

Conflict of Interest

The authors declare no conflict of interest.

Data Availability Statement

The data that support the findings of this study are available in the supplementary material of this article.

Keywords: iodine · sulfur trioxide · polyiodide · oxoanion · crystal structure

- [1] M. H. Klaproth, *Phil. Mag.* **1798**, *1*, 78.
[2] G. Magnus, *Ann. Phys.* **1827**, *10*, 491.
[3] D. J. Prince, J. D. Corbett, B. Garbisch, *Z. Anorg. Chem.* **1970**, *9*, 2731.
[4] R. K. Mullen, D. J. Price, J. D. Corbett, *Z. Anorg. Chem.* **1971**, *10*, 1749.
[5] R. J. Gillespie, J. Passmore, *Adv. Inorg. Chem. Radiochem.* **1975**, *17*, 49.
[6] R. J. Gillespie, *J. Chem. Soc.* **1979**, *8*, 315.
[7] I. D. Brown, D. B. Crump, R. J. Gillespie, *Inorg. Chem.* **1971**, *10*, 2319.
[8] I. Masson, C. Argument, *J. Chem. Soc.* **1938**, 1702.
[9] C. G. Davies, J. R. Gillespie, P. R. Irel, J. M. Sowa, *Can. J. Chem.* **1974**, *52* (11), 2048.
[10] J. Passmore, P. Taylor, T. Whidden, P. S. White, *Can. J. Chem.* **1979**, *57*, 968.
[11] J. Passmore, G. Sutherland, P. S. White, *Inorg. Chem.* **1981**, *20*(7), 2169.
[12] A. Appleby, F. Grein, J. P. Johnson, J. Passmore, P. S. White, *Inorg. Chem.* **1986**, *25*, 422.
[13] J. D. Corbett, *Prog. Inorg. Chem.* **1976**, *21*, 129.
[14] C. Chung, G. H. Cady, *Inorg. Chem.* **1972**, *11*, 2528.
[15] R. J. Gillespie, K. C. Malhotra, *Inorg. Chem.* **1969**, *8*, 1751.
[16] R. J. Gillespie, J. B. Milne, M. J. Morton, *Inorg. Chem.* **1968**, *7*, 2221.
[17] R. Faggiani, R. J. Gillespie, R. Kapoor, C. J. L. Lock, J. E. Vekris, *Inorg. Chem.* **1988**, *27*, 4350.
[18] W. Gottardi, *Mh. Chemie* **1975**, *106*, 1203.
[19] A. Bali, K. C. Malhotra, *J. Inorg. Nucl. Chem.* **1976**, *38*, 411.
[20] J. Bruns, T. Klüner, M. S. Wickleder, *Angew. Chem. Int. Ed.* **2013**, *52*, 2590; *Angew. Chem.* **2013**, *125*, 2650.
[21] J. Bruns, M. Hänsch, M. S. Wickleder, *Inorg. Chem.* **2015**, *54*, 5681.
[22] J. Bruns, T. Klüner, M. S. Wickleder, *Chem. Asian J.* **2014**, *9*, 1594.
[23] J. Bruns, O. Niehaus, R. Pöttgen, M. S. Wickleder, *Chem. Eur. J.* **2014**, *20*, 811.
[24] S. Schwarzer, A. Betke, C. Logemann, M. S. Wickleder, *Eur. J. Inorg. Chem.* **2017**, *3*, 752.
[25] M. Pley, M. S. Wickleder, *Eur. J. Inorg. Allg. Chem.* **2005**, *630*, 529.
[26] M. Pley, M. S. Wickleder, *Angew. Chem.* **2004**, *116*, 4262; *Angew. Chem. Int. Ed.* **2004**, *43*, 4168.
[27] A. Arndt, M. S. Wickleder, *Z. Anorg. Allg. Chem.* **2006**, *632*, 2104.
[28] M. Pley, M. S. Wickleder, *Z. Anorg. Allg. Chem.* **2004**, *630*, 1753.
[29] J. Bruns, D. van Gerven, T. Klüner, M. S. Wickleder, *Angew. Chem.* **2016**, *128*, 8253; *Angew. Chem. Int. Ed.* **2016**, *128*, 8121.
[30] J. Bruns, M. Eul, R. Pöttgen, M. S. Wickleder, *Angew. Chem. Int. Ed.* **2012**, *51*, 2204.
[31] L. V. Schindler, M. Struckmann, A. Becker, M. S. Wickleder, *Eur. J. Inorg. Chem.* **2017**, *5*, 958.
[32] L. V. Schindler, A. Becker, M. Wieckhusen, T. Klüner, M. S. Wickleder, *Angew. Chem.* **2016**, *128*, 16399; *Angew. Chem. Int. Ed.* **2016**, *55*, 16165.
[33] I. A. Koppel, P. Burk, I. Koppel, I. Leito, T. Sonoda, M. Mishima, *J. Am. Chem. Soc.* **2000**, *122*, 5114.
[34] R. Grau, W. A. Roth, *Z. Anorg. Allg. Chem.* **1930**, *188*, 173.
[35] M. Daub, K. Kazmierczak, P. Gross, H. A. Höpfe, H. Hillebrecht, *Inorg. Chem.* **2013**, *52*, 6011.
[36] M. Daub, K. Kazmierczak, H. A. Höpfe, H. Hillebrecht, *Chem. Eur. J.* **2013**, *19*, 16954.
[37] P. Netzsch, H. A. Höpfe, *Eur. J. Inorg. Chem.* **2021**, *11*, 1065.
[38] S. Sutorius, D. van Gerven, S. Olthof, B. Rasche, J. Bruns, *Chem. Eur. J.* **2022**, *28*, e202200004.
[39] J. Passmore, G. Sutherland, T. Whidden, P. S. White, *J. Chem. Soc. Chem. Commun.* **1982**, 289.
[40] M. P. Murchie, J. P. Johnson, J. Passmore, G. W. Sutherland, M. Tajik, T. K. Whidden, P. S. White, F. Grein, *Inorg. Chem.* **1992**, *31*, 273.
[41] S. Brownridge, I. Krossing, J. Passmore, H. D. B. Jenkins, H. K. Roobottom, *Coord. Chem. Rev.* **2000**, *197*, 397.
[42] C. Logemann, T. Klüner, M. S. Wickleder, *Angew. Chem. Int. Ed.* **2012**, *51*, 4997.
[43] Bruker (2018). Apex3. Bruker AXS Inc., Madison, Wisconsin, USA.
[44] G. Sheldrick, *Acta Crystallogr. Sect. A* **2015**, *71*, 3.

Manuscript received: May 25, 2022

Revised manuscript received: June 26, 2022